Equilibrium Constant for Water Dimerization: Analysis of the Partition Function for a Weakly Bound System

ARTICLE *in* THE JOURNAL OF PHYSICAL CHEMISTRY A · FEBRUARY 2002

Impact Factor: 2.69 · DOI: 10.1021/jp0129131

3 AUTHORS:

Gregory K Schenter
Pacific Northwest National Laboratory
203 PUBLICATIONS **4,450** CITATIONS
SEE PROFILE

Shawn M Kathmann
Pacific Northwest National Laboratory
83 PUBLICATIONS **1,099** CITATIONS
SEE PROFILE

Bruce C Garrett
Pacific Northwest National Laboratory
296 PUBLICATIONS **11,892** CITATIONS
SEE PROFILE

Equilibrium Constant for Water Dimerization: Analysis of the Partition Function for a Weakly Bound System

Gregory K. Schenter, Shawn M. Kathmann, and Bruce C. Garrett*

Environmental Molecular Sciences Laboratory, Pacific Northwest National Laboratory, Richland, Washington 99352

Received: July 27, 2001; In Final Form: November 9, 2001

The treatment of dissociative states in the calculation of the partition function of a weakly bound system, such as the water dimer, is discussed. For a dissociative system, the number of phase-space configurations that contribute to the total partition function from energies above the dissociation energy depends on the system volume. For a sufficiently large system volume, entropy from these configurations will dominate over the energy contribution of the local minimum and contributions from dissociative states will dominate the total partition function. The calculation of the dimer partition function requires limiting the phase space of the cluster or providing a definition of those phase-space points that correspond to a dimer. Because there is no unique procedure to constrain the phase space of a dimer, we provide an analysis of the dimer partition function using a series of constraints. For the water dimer at temperatures in the range 200−500 K, the values of the dimer partition function change by over 2 orders of magnitude depending on the choice of the constraint.

1. Introduction

The role of water dimers in the atmosphere has received considerable attention,[1−4] yet their equilibrium population remains uncertain.[3−5] The water dimer is a relatively weakly bound complex, and thus, its thermodynamic properties are difficult to determine experimentally. For example, significant variations are found in the observed values of the dimer enthalpy of formation determined using different techniques.[6] Theoretical determination of the thermodynamic properties of the water dimer (e.g., the equilibrium constant for dimerization) persists as an active area of research.[1,4,5,7−9]

A recent publication in this journal[9] reported impressive calculations of the vibrational energy levels up to near the dissociation of the water dimer for a very accurate potential energy surface.[10,11] These energy levels were then used in calculations of the dimer partition function and the dimerization equilibrium constant as a function of relative humidity for temperatures ranging from about 25 to 130 °C. From these calculations, the authors concluded that "it is probable that the water dimer can be indeed present in the atmosphere in sufficient quantities to have significant effects on solar absorption." Although these calculations represent the most accurate determination of energy levels to date, the authors did not discuss the role of dissociative states of the weakly bound water dimer on the dimer partition function in their study. In a recent study,[8] it was shown that the enthalpy of formation of the water dimer at 85 °C can change by over 10 kJ/mol depending upon how dissociative states are treated. Upon the basis of our previous work calculating the thermodynamics and kinetics of clusters relevant to the nucleation process,[12,13] we found that the treatment of dissociative states can affect the computed partition functions and equilibrium constants for the water dimer, particularly at higher temperatures. For example, if the free energy of dimerization displays similar changes, as does the dimerization enthalpy, e.g., 10 kJ/mol, then different treatments of dissociative states can shift the equilibrium constant by over a factor of 30. The purpose of this work is to take a closer look at the role of dissociative states on the computed partition function and to provide an estimate of the change in the partition function, which determines the equilibrium constant, for different treatments of these states.

One way to understand the effects of dissociative states on thermodynamic properties of the dimer is to write the partition function, $Q(T)$, for the dimer in terms of a convolution of the density of rovibrational states, $\rho(E)$, and the Boltzmann factor as

$$Q(T) = \int_0^\infty \mathrm{d}E\, \mathrm{e}^{-\beta E}\, \rho(E) \tag{1}$$

where T is temperature, E is the total energy (relative to the energy at the equilibrium geometry of the dimer), $\beta = 1/(k_B T)$, and k_B is Boltzmann's constant. If we treat rotations of the dimer by the rigid rotor approximation and vibrations harmonically, the classical density of states (DOS) scales as $E^{s+1/2}$, where s is the number of active vibrations in the dimer. (Vibrational modes with sufficiently high frequencies will not contribute appreciably to the quantum mechanical DOS and are often not included in the number of vibrational modes.) The rigid rotor harmonic oscillator (RRHO) approximation provides a qualitatively correct description of the dependence of $\rho(E)$ on energies below dissociation. For energies above dissociation, the DOS scales linearly with the total volume of the system. Figure 1 depicts the behavior of the Boltzmann factor, DOS, and their product (the integrand of eq 1) for energies below dissociation. For the lower temperature (dashed curves in Figure 1), the integrand

* To whom correspondence should be addressed. E-mail: bruce.garrett@pnl.gov. Phone: (509) 376-1353. Fax: (509) 376-0420.

10.1021/jp0129131 CCC: $22.00
Published on Web 01/29/2002

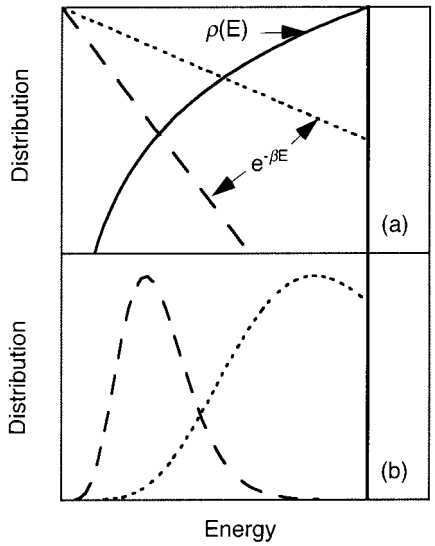

Figure 1. Logarithmic plot of $(E/D)^{s-1}$ (solid line) for $s = 7.5$ and Boltzmann factors, $e^{-\beta E}$ (dashed and dotted lines), for two values of $\beta = 1/k_B T$, as a function of energy E from zero to D (a). The vertical line is at $E = D$. Part b shows the linear plot of $(E/D)^{s-1}\ e^{-\beta E}$ (normalized to one at its maximum) for two values of β. The dashed (dotted) curves in parts a and b are for the lower (higher) values of temperature, T.

peaks well below the dissociation energy and the population is negligible for energies near but below the dissociation energy. For the higher temperature (dotted curves in Figure 1), the integrand peaks very close to the dissociation energy and has an appreciable value at dissociation. For a sufficiently large volume, the total partition function will be dominated by configurations with energies above dissociation; that is, entropy from these configurations will dominate over the energy contributions of the local minima. However, many of the states above dissociation could not be characterized as dimers (e.g., they may correspond to collision complexes or resonances that are too short lived to contribute to any physically observable property of the dimer). For the lower temperature, the clear separation of the distribution below dissociation from that above dissociation makes it easy to determine what energies should contribute to the dimer partition function. Even though dissociative states are ultimately the most probable (for a large enough system volume), the dimer is sufficiently stable at the low temperature (i.e., there is no appreciable probability of being at energies close to but below dissociation) that the time scale to achieve the most probable (dissociated) states is long compared to any observation of dimer properties. For the higher temperature, it is not immediately obvious what role dissociative states should play in the dimer partition function. The large distribution of states near dissociation at the higher temperature is a measure of the instability of the dimer at this temperature, and it is possible that some states above dissociation will be sufficiently long-lived to contribute to dimer properties.

Calculation of the dimer partition function requires limiting the phase space of the two molecules, which is equivalent to providing a functional definition of the dimer. Most often this constraint is implicit in the calculation. For example, in quantum mechanical calculations of the partition function using the RRHO approximation, the dissociative continuum is discretized by extending the harmonic representation of the potential above dissociation, thereby converging the vibrational partition function. Most previous calculations of the water dimer partition function have employed this approximation. Accurate quantum mechanical calculations on polyatomic systems are now possible, which allow determination of bound energy levels beyond the harmonic approximation.[9,10,14,15] The question still arises of how to treat the dissociative continuum. Goldman et al.[9] have limited their calculations of the water dimer partition function to energies below dissociation, thereby imposing an energetic constraint. Christoffel and Bowman[15] computed energy levels above dissociation for the HCO_2 system using an approximate expression for the potential through three-mode coupling in normal mode coordinates. This approximate form for the potential could also effectively constrain the phase space to effectively discretize the continuum.

The definition of a molecular cluster has long been recognized as an important issue in molecular theories of gas-to-liquid homogeneous nucleation, because clusters that contribute to nucleation are inherently unstable.[12,13,16−19] In these approaches, the constraints are often geometric ones. For example, "physically consistent" clusters[18] are defined such that all molecules in the cluster lie within a spherical volume centered on the center of mass of the cluster. Stillinger provided an alternate geometric definition that requires each molecule to lie within a specified distance of another molecule in the cluster.[16]

The dimer partition function is an important component in the construction of rate theories for unimolecular reactions, such as cluster dissociation reactions that are important in nucleation. Dissociative states should be included in the reactant partition function for the evaluation of unimolecular rate constants because these states are the ones that lead to reaction. In practice, separate calculations are performed for the reactive flux and reactant partition function, and the reactant partition function could be approximated by only bound-state contributions, although this would be inconsistent with the treatment of dissociative states in the reactive flux calculation. For a unimolecular reaction with a barrier, a dividing surface through the saddle point for the reaction provides a convenient separation of the configuration space into reactants (dimers) and products (monomers). This definition of the dimer is implicit in conventional forms of transition state theory (TST),[20] which is used in the Rice−Ramsperger−Kassel−Marcus (RRKM) theory[21] of unimolecular reactions, and explicitly displayed in formulations of transition state theory in terms of time correlation functions.[22] Definition of dimer partition functions for dissociation of the water clusters is made difficult by the lack of an intrinsic barrier to reaction (i.e., the potential energy is monotonically downhill in energy for a water molecule recombining with a cluster). In this case, variational transition state theory[23] can be used to define the optimum dividing surface separating reactants from products.[12,13] Most calculations do not apply this type of constraint though because the reactant partition function is calculated using the harmonic approximation. One exception is the accurate classical evaluation of the reactant phase space bounded by the reaction coordinate of the variational transition state for the H_3^+ dissociation.[24]

Constraints on the energy can also be used to avoid divergence of the partition function. As noted above, Goldman et al.[9] effectively replaced the upper limit of integration in eq 1 by the dissociation energy, D. This constraint will be most appropriate for properties for which the low-lying energy levels dominate the average. For example, it is possible that high-lying states may not contribute appreciably to absorption over narrow frequency ranges (such as those near the shifted donor OH stretch in the water dimer). This total energy constraint excludes all states that are above the dissociation energy. Orbiting resonances, which correspond qualitatively to states with vibrational energy below dissociation and total energy

(vibrational plus rotational) above dissociation, can be long-lived, indicating a relatively weak coupling to dissociative modes in the complex, and therefore, it may be important to include these types of states in some averages. This suggests that an energy constraint on vibrational energy may be more appropriate than one on total energy. Similarly, there may be some vibrational modes that couple weakly to dissociative modes of the complex and therefore support long-lived excitations. In this case, a constraint on only the subset of dissociative modes may be more appropriate.

The use of the lifetime of dissociative (resonance) states to understand their contributions to the partition function arises naturally out of the preceding discussion. Rather than assigning constraints based upon energy content of certain modes, the lifetime of individual resonance states could be used to determine whether the energy level should be included in the partition function. An effective Hamiltonian formulation has been used to model quantum mechanically the intramolecular dynamics that controls the lifetimes of energy levels.[25] Alternatively, classical trajectories can be used to evaluate the lifetime of points in phase space. This latter approach was used in calculations of the water dimerization enthalpy.[8] In this previous work, the time for water dimers, at energies above dissociation, to dissociate (i.e., for the intermolecular separation to increase beyond a limit) was used to determine whether the state should be included in the average. The relationship between collision lifetimes and thermodynamic functions was first recognized by Smith.[26] In this seminal paper, it was noted that the concentration of an unstable complex is given by the product of its rate of formation (i.e., the collision frequency) and its lifetime, and a general expression was derived that related the lifetime matrix[27] to the "molecular internal partition function". Contributions from the collisional continuum are included in terms of the difference between the lifetime of a collision and the time for motion of the particles in the absence of the interaction (i.e., with the potential turned off). In this approach, a convergent expression is obtained for the partition function without the need to introduce additional parameters such as cutoff energies or distances. The relationship between the DOS and the collision lifetime, which is implicit in Smith's work, has also been explicitly displayed[28] (see also Brumer et al.[29] and references therein). It should also be noted that the collision lifetime has played an important role in derivation of rate expressions for recombination reactions.[30] Although an approach based upon the lifetime matrix is conceptually compelling, it requires full solution of the collision dynamics. Evaluation of the lifetime matrix has been carried out for reactions involving a small number of atoms (for a recent example, see the calculations for the $H + O_2$ reaction by Pack et al.[31]).

In the present work, we analyze the partition function calculations for the water dimer, first, to explore the effects of energetic and geometric constraints on the partition functions. Second, we examine what contributions are made by dissociative states in the approaches used in the literature. We use the interaction potential of Dang and Chang,[32] which provides a reasonable description of water interactions with accurate binding energies and intermolecular vibrational frequencies. In this model, the monomers are treated as rigid bodies (i.e., no internal vibrations of the monomers), and thus, contributions from intramolecular modes are not explicitly included in our partition functions. The effects of coupling between the intermolecular and intramolecular vibrational modes are included implicitly in the energetics because these models were parametrized empirically. For example, the effects of shifts in the OH vibrational frequency upon forming a hydrogen bond are included in some average sense. However, effects of the coupling on dynamics, such as lifetimes of resonances, will not be included, even implicitly. It can be argued that the frequency mismatch between the high-frequency intramolecular modes and the lower-frequency intermolecular modes will decrease dynamic coupling between these sets of modes. The goal of this work is to provide a qualitative understanding of the effects of dissociative states and not to provide quantitative estimates of thermodynamic properties. Therefore, the use of this approximate model of the water−water interaction will be sufficient for this study.

Section 2 and Appendices A and B present explicit expressions for the density of states and partition functions so that the effects of the different constraints are clearly displayed. Section 3 presents the results and a discussion of the effects of the different constraints. Section 4 presents a summary and conclusions.

2. Theory and Calculational Details

Four constraints on the phase space of the dimer are considered: (i) the available phase space is restricted to those states with total energies below the dissociation energy, D; (ii) the available phase space is restricted to those states with energies in k vibrational modes below D, where k can take on values from 1 to the total number of vibrational modes; (iii) configuration space is constrained so that vibrational motion is restricted to lie within the turning points of the harmonic approximation to the potential; (iv) configuration space is constrained so that the center-of-mass separation between the two water molecules is restricted to be less than the distance R_{CUT}. The first two constraints are energetic ones, and the last two are geometric ones. We do not explicitly consider any constraints based upon lifetimes of dissociative states in this paper, although the energetic constraints can be qualitatively related to assumed lifetimes. Constraint (i) is equivalent to assuming that all states above dissociation couple strongly to the dissociative mode and their lifetimes are sufficiently short so that they will not contribute appreciably to the partition function. Constraint (ii) relaxes this restriction and is equivalent to assuming that some modes couple weakly to the dissociative mode and they are sufficiently long-lived that they contribute to the partition function. By considering a range of energy constraints (e.g., number of modes included in the constraint), we can span a range of possible behaviors of the lifetimes of the states. These constraints are first defined in terms of the classical density of states. Although a classical description of the water dimer is not valid at energies corresponding to low-lying bound states, it should be a reasonable approximation for describing the DOS at energies near and above dissociation.

In this section, we describe accurate classical simulations of the classical DOS and partition functions for the coupled vibrational and rotational degrees of freedom. We also consider an approximate treatment of the vibrations and rotations that allows us to explore the effects of the different constraints. The rotations and vibrations are treated as separable in the approximate treatment with rotations treated as those for a rigid asymmetric top and vibrations treated in the harmonic approximation. The extension of these constraints to quantum mechanical calculations of the DOS and partition functions are then presented for the first three of these constraints using the rigid rotor harmonic oscillator (RRHO) approximation.

A. Classical Density of States and Partition Function. The classical partition function is given by eq 1 with the classical

anharmonic (CA) density of states for rotations and vibrations given by

$$\rho^{y}_{\mathrm{CA}}(E) = \frac{1}{h^N}\int \mathrm{d}\mathbf{p}\ \mathrm{d}\mathbf{q}\ \delta[E - H(\mathbf{q},\mathbf{p})] f_y(\mathbf{q},\mathbf{p}) \qquad (2)$$

where h is Planck's constant, N is the number of vibrational and rotational degrees of freedom in the system, $\mathbf{q}$ and $\mathbf{p}$ are the coordinate and conjugate momentum vectors for vibrations and rotations, $\delta(x)$ is the Dirac delta function, $H(\mathbf{q},\mathbf{p})$ is the total Hamiltonian for the system, and $f_y(\mathbf{q},\mathbf{p})$ is the constraint function that limits the phase-space integration. The quantities that are computed classically using the rigid rotor harmonic oscillator (RRHO) approximation are denoted by replacing the subscript CA by CH in expressions for the classical DOS and partition function.

The first constraint (total energy constrained below dissociation, $y = D$) is easily applied to both the anharmonic and RRHO treatments by defining the constraint function as

$$f_D(\mathbf{q},\mathbf{p}) = \theta[D - H(\mathbf{q},\mathbf{p})] \qquad (3)$$

where $\theta(x)$ is a Heaviside step function [$\theta(x) = 0$, $x < 0$; $\theta(x) = 1$, $x > 0$]. With this constraint, the DOS and partition function (for the rotational and vibration coordinates) are denoted by $\rho^{D}_{\mathrm{CA}}(E)$ and $Q^{D}_{\mathrm{CA}}(T)$, when the system is treated anharmonically, or they are denoted by $\rho^{D}_{\mathrm{CH}}(E)$ and $Q^{D}_{\mathrm{CH}}(T)$ in the RRHO approximation.

The second constraint (vibrational energy constrained below dissociation, $y = D\upsilon k$) requires a separation of the rotational and vibrational degrees of freedom, so its use is restricted to the RRHO approximation. The constraint is imposed using the function

$$f_{D\upsilon k}(\mathbf{q},\mathbf{p}) = \theta[D - H_{\upsilon k}(\mathbf{q},\mathbf{p})] \qquad (4)$$

where $H_{\upsilon k}$ is the approximate harmonic Hamiltonian for k vibrational modes. Note that for the classical calculations it is not necessary to specify which modes are constrained because the DOS depends only on the number of modes k that are constrained. Again, this constraint is implemented only when the DOS is calculated in the RRHO approximation. The DOS and partition function are denoted by $\rho^{D\upsilon k}_{\mathrm{CH}}(E)$ and $Q^{D\upsilon k}_{\mathrm{CH}}(T)$, respectively.

The third constraint (coordinates constrained within turning points of the harmonic approximation to the potential, $y = \mathrm{HO}$) is implicitly imposed by assuming that the functional form for the DOS in the RRHO approximate model can be extended to energies above dissociation. This approach can naturally be applied to the RRHO calculations and is generally the approach used in the literature. We also extend this approach to the anharmonic calculations by fitting the numerically calculated DOS for energies below dissociation to the RRHO functional form, which is used to extend $\rho(E)$ above D. With this constraint, the DOS and partition function are denoted by $\rho^{\mathrm{HO}}_{\mathrm{CA}}(E)$ and $Q^{\mathrm{HO}}_{\mathrm{CA}}(T)$, when the system is treated anharmonically, or by $\rho^{\mathrm{HO}}_{\mathrm{CH}}(E)$ and $Q^{\mathrm{HO}}_{\mathrm{CH}}(T)$ in the RRHO approximation.

The fourth constraint (center-of-mass separation constrained below R_{CUT}, $y = R$) is imposed using the function

$$f_R(\mathbf{q},\mathbf{p}) = \theta[R_{\mathrm{CUT}} - R_{\mathrm{CM}}] \qquad (5)$$

where R_{CM} is the center-of-mass separation of the two water molecules and R_{CUT} is a constant. This constraint has been used extensively in molecular theories of gas-to-liquid nucleation and has been termed the physically consistent cluster.[17,18] We have used this approach previously in anharmonic calculations on water clusters.[12,13] In the current work, we employ this approach only for calculating the partition functions, $Q^{\mathrm{R}}_{\mathrm{CA}}(T)$.

The water monomers in our calculations are treated as rigid. When three intramolecular vibrational degrees of freedom for each monomer and three center-of-mass degrees of freedom for the dimer are removed, the number of degrees of freedom is nine ($N = 9$) corresponding to six intermolecular vibrations and three rotations of the dimer. Explicit analytical expressions for RRHO DOS and partition functions without constraints are available in textbooks.[21] Appendix A reviews these expressions and presents extensions to the constraints discussed above. Accurate anharmonic calculations of the DOS for the first constraint in eq 3, $\rho^{D}_{\mathrm{CA}}(E)$, are obtained numerically using a multiple histogram method similar to that used by Weerasinghe and Amar.[33] A series of canonical ensemble simulations were performed by using a Metropolis Monte Carlo procedure to generate the distributions, $\mathrm{e}^{-\beta E}\,\rho(E)$, as a function of total energy at temperatures of 10, 20, 30, 40, 50, 100, 150, and 200 K. The total energy at each phase-space configuration is obtained by sampling phase-space configurations for the effective Hamiltonian

$$H_{\mathrm{eff}} = V(q) + {}^1/_2 \sum_{i=1}^{N} k_{\mathrm{B}} T \xi_i^{\,2} \qquad (6)$$

where ξ_i is a Gaussian-distributed random variable with unit standard deviation and $N = 9$. A total of 10^5 Monte Carlo moves were sampled for each temperature. The Monte Carlo procedure was initiated with a minimum energy configuration so that there was sufficient sampling of configurations with $E < D$. The energy was binned in the range $0 < E < D$ to obtain an unnormalized distribution, $C\ \mathrm{e}^{-\beta E}\,\rho(E)$. Distributions for the various temperatures were matched to recover an unnormalized distribution across the full energy range. The methods used in the calculations of the partition functions with the fourth geometric constraint are provided elsewhere.[13]

B. Quantum Mechanical Density of States and Partition Function. The quantum mechanical density of states and partition function can be expressed in terms of the discrete energy levels of the system. Although Goldman et al. have calculated accurate (anharmonic) vibrational energy levels,[9] those calculations are computationally intensive, and the rigid rotor harmonic oscillator treatment presented here will allow us to demonstrate the effect of the different constraints. The energetic constraints listed above ($y = D$ and $y = D\upsilon k$) can be easily implemented in quantum mechanical calculations by including only those energy levels that obey the constraints in the calculations of the DOS and partition function. For the RRHO approximation, the implicit harmonic constraint ($y = \mathrm{HO}$) is also easily implemented in the quantum mechanical calculations.

As noted by Goldman et al.,[9] the B and C components of the principle moment of inertia of the water dimer are approximately equal ($I_{\mathrm{B}} \approx I_{\mathrm{C}}$), so it is a good approximation to treat the water dimer as a prolate symmetric top. In this case, the rotational energy levels and degeneracies are given by

$$\epsilon^{\mathrm{r}}_{JK} = BJ(J+1) + (A - B)K^2$$
$$g_{JK} = (2J+1)(2 - \delta_{K,0}) \qquad (7)$$

where $\delta_{\mathrm{KK}'}$ is the Kronecker delta function and in our imple-

TABLE 1: Parameters Used in Rigid Rotor Harmonic Oscillator Calculations

ω_m (cm^{-1})[a]	127.0 (A')	220.2 (A')	405.3 (A')	108.4 (A'')	168.5 (A'')	619.6 (A'')
I_A, I_B, I_C (au)	15 840	492 600	493 400			
A, B (cm^{-1})	6.929	0.2226				
D (cm^{-1})	1640					

[a] Symmetries of the vibrational modes are given in parentheses.

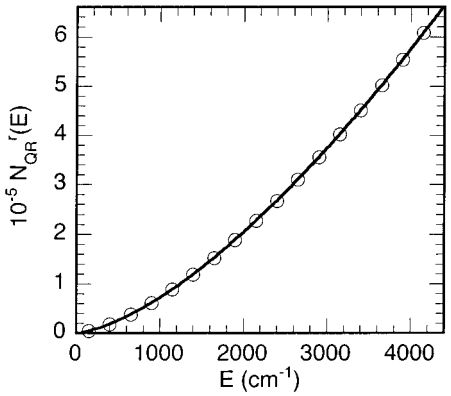

Figure 2. Comparison of classical (symbols) and quantum mechanical (curve) rotational number of states.

mentation the rotational constants are defined by

$$A = \frac{\hbar^2}{2I_A}$$

$$B = \frac{\hbar^2}{I_B + I_C} \tag{8}$$

where values of the constants are given in Table 1. Given the analytical expressions for the vibrational and rotational energy levels, the DOS and partition function can be written in terms of explicit sums over these energy levels. The partition function with no constraints takes the standard form for the RRHO approximation.[21] Appendix B reviews these expressions. We note that although the classical DOS with this constraint depends only on the number of modes k that are constrained, for the quantum mechanical DOS it is necessary to specify which modes are constrained.

There are over 150 000 rotational energy levels for energies below dissociation, and when combined with the vibrational states, there are over 10^7 energy levels for $E < D$. We are also interested in extending the calculations to energies well above dissociation, where the number of states is much larger and a direct sum over energy levels is impractical. The large number of rotational states indicates that a classical approximation to the rotational DOS and partition function might be accurate. We examine the validity of the classical approximation for rotations within the rigid rotor approximation by examining the number of rotational states as given by eqs B.10 and B.11. The comparison of N_{QR}^{r} and N_{CR}^{r} is shown in Figure 2. The excellent agreement between these quantities indicates that a classical treatment of the rotational number of states and DOS is valid. Appendix B also reviews expressions for the RRHO DOS and partition function with a mixed treatment (quantum mechanics for vibrations and classical mechanics for rotations). We use the mixed expression for the DOS (quantum mechanical for vibrations and classical for rotations), which is given in eq B.12, to examine the effects of the energy constraints on the quantum mechanical partition function.

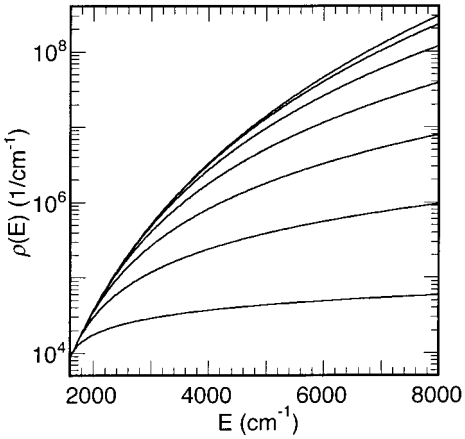

Figure 3. Calculated classical rigid rotor harmonic oscillator density of states for the water dimer using the Dang−Chang interaction model. The topmost curve is the harmonic oscillator approximation to the DOS with the harmonic oscillator constraint above dissociation, $\rho_{CH}^{HO}(E)$. The lower curves represent the DOS with the vibrational energy constraint $\rho_{CH}^{Dvk}(E)$, with $k = 1-6$. At a fixed energy, $\rho_{CH}^{Dvk}(E)$ monotonically decreases with increasing k and the results for $k = 1$ are closest to those for the harmonic oscillator constraint.

3. Results and Discussion

The parameters used in the rigid rotor harmonic calculations are listed in Table 1. Also, note that the dissociation energy that we use in these calculations, 1640 cm^{-1}, is relative to the bottom of the classical well (i.e., without contribution from zero-point energy). Figure 3 compares the classical RRHO DOS for the Dvk constraint with different values of k. The results for $\rho_{CH}^{Dvk}(E)$ show a range of behavior, with $k = 6$ giving the greatest decrease in the DOS for energies above dissociation and with $k = 1$ giving results that are very close to the $\rho_{CH}^{HO}(E)$ values for energies up to 5 times the dissociation energy.

The frequencies of the six intermolecular modes of the water dimer are shown in Table 1. We number the modes in the order that they appear in the table. Note that the frequencies are listed by symmetry block and in increasing order within each block. For the Dang−Chang potential, the equilibrium geometry of the water dimer has C_s symmetry and the dissociative mode, corresponding qualitatively to an O−O stretch, has A' symmetry and a frequency of 220 cm^{-1}. We expect vibrational modes to couple more strongly with modes of the same symmetry; therefore, for the remainder of the calculations, we report the results with the Dvk constraint with $k = 3$ and 6 only. In the quantum mechanical calculations with $k = 3$, the three modes are taken to be those with A' symmetry. As shown in Figure 3, the HO constraint and the Dvk constraint with $k = 3$ and 6 will give an adequate sampling of the range of behavior of the DOS above dissociation.

The main results of this work are the calculated densities of states as a function of energy, which are summarized in Figures 4 and 5, and the corresponding partition functions, which are presented in Table 2 and Figure 6. Figure 4a shows the classical rovibrational DOS that are calculated using the anharmonic potential and the RRHO approximation with the first three constraints, and Figure 5a shows the quantum mechanical

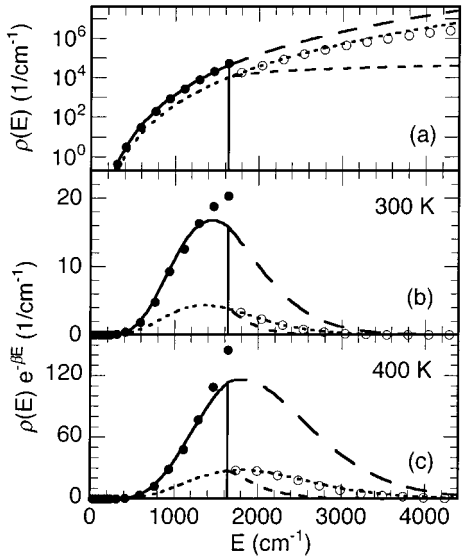

Figure 4. Calculated classical rovibrational density of states for the water dimer using the Dang−Chang interaction model. Part a displays the DOS, and parts b and c show the product of the DOS with the Boltzmann factor at 300 and 400 K, respectively. The solid circles are the accurate anharmonic results, $\rho^D_{CA}(E)$, the solid curve is a linear fit to ln $\rho^D_{CA}(E)$ vs ln E, for energies below the dissociation energy, and the long-dash curve is the extrapolation of the accurate DOS above dissociation using the harmonic oscillator approximation, $\rho^{HO}_{CA}(E)$. The dotted curve is the RRHO DOS with the harmonic oscillator constraint above dissociation, $\rho^{HO}_{CH}(E)$, the short-dash curve is the RRHO DOS with vibrational energy constrained in all modes above dissociation, $\rho^{D\upsilon k}_{CH}(E)$ ($k = 6$), and the open circles are the RRHO DOS with vibrational energy constrained in three modes above dissociation, $\rho^{D\upsilon k}_{CH}(E)$ ($k = 3$).

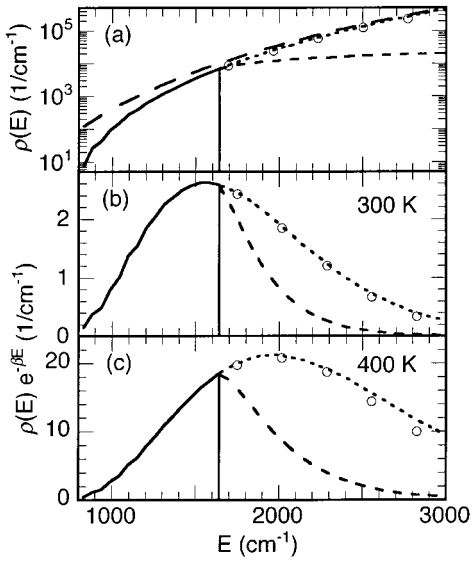

Figure 5. Calculated quantum mechanical rovibrational density of states for the water dimer using the Dang−Chang interaction model. Part a displays the DOS, and parts b and c show the product of the DOS with the Boltzmann factor at 300 and 400 K, respectively. The solid line is the harmonic oscillator approximation below the dissociation energy, $\rho^D_{QH}(E)$, the dotted curve is the RRHO DOS with the harmonic oscillator constraint above dissociation, $\rho^{HO}_{QH}(E)$, the short-dashed curve is the RRHO DOS with vibrational energy constrained in all modes above dissociation, $\rho^{D\upsilon k}_{QH}(E)$ ($k = 6$), and the open circles are the RRHO DOS with vibrational energy constrained in three modes above dissociation, $\rho^{D\upsilon k}_{QH}(E)$ ($k = 3$). For comparison, the classical harmonic DOS $\rho^{HO}_{CH}(E)$ is shown as the long-dashed curve.

rovibrational DOS calculated using the RRHO approximation with the first three constraints. Parts b and c of Figures 4 and 5 show the product of the DOS with the Boltzmann factor at 300 and 400 K, respectively. The classical RRHO DOS with the HO constraint is also shown in Figure 5 for comparison. The classical anharmonic DOS is higher than the classical RRHO DOS at the dissociation energy by a factor of 5.3. The numerical calculations of $\rho^D_{CA}(E)$ only determine the quantity to within an arbitrary scaling factor. The absolute value of $\rho^D_{CA}(E)$ is determined by setting $\rho^D_{CA}(E)$ equal to $\rho^D_{CH}(E)$ at the lowest energy for which $\rho^D_{CA}(E)$ was calculated, namely, 31 cm^{-1}. The classical RRHO DOS scales as $E^{6.5}$, whereas a linear least-squares fit of ln$[\rho^D_{CA}(E)]$ vs ln(E) gives a slope of 6.93, giving rise to a value of $\rho^D_{CA}(E)$ that is over 5 times larger than $\rho^D_{CH}(E)$ at $E = D$. The classical anharmonic results are extrapolated to energies above dissociation using the HO constraint with the expression $\rho^{HO}_{CA}(E) = \rho_D(E/D)^{6.5}$ where ρ_D is the value of the linear least-squares fits of ln$[\rho^D_{CA}(E)]$ vs ln(E) evaluated at $E = D$.

As shown in Figures 4 and 5, the total energy constraint ($y = D$) is the most restrictive followed by the vibrational energy constraint ($y = D\upsilon k$) and the harmonic oscillator constraint (y = HO) to give $\rho^D_{CH}(E) \le \rho^{D\upsilon k}_{CH}(E) \le \rho^{HO}_{CH}(E)$ and $\rho^D_{QH}(E) \le \rho^{D\upsilon k}_{QH}(E) \le \rho^{HO}_{QH}(E)$, where the equality holds for energies below dissociation. As temperature is increased, the contribution to the partition function from energies above dissociation increases for the vibrational energy constraint and harmonic oscillator constraint. Figures 4 and 5 also show that the maximum in the $\rho(E)$ $e^{-\beta E}$ distribution for both the classical and quantum densities of states with the harmonic oscillator constraint is below dissociation at 300 K but moves to an energy above dissociation at 400 K, so a *significant contribution to the partition function comes from energies above dissociation.* One measure of the contribution to the partition function from energies above dissociation is the ratio of the partition function with the vibrational energy or harmonic oscillator constraint to the partition function with the total energy constraint, which has no contribution from energies above dissociation. The ratio $Q^{D\upsilon k}_{CH}(T)/Q^D_{CH}(T)$ with $k = 6$ increases from 1.1 to 2.3 as the temperature increases from 200 to 500 K, and the ratio $Q^{HO}_{CH}(T)/Q^D_{CH}(T)$ increases from 1.1 to 6.8 as the temperature increases from 200 to 500 K. Similarly, $Q^{D\upsilon k}_{QH}(T)/Q^D_{QH}(T)$ and $Q^{HO}_{QH}(T)/Q^D_{QH}(T)$ increase from 1.2 to 2.8 and from 1.2 to 11.1, respectively, as the temperature increases from 200 to 500 K.

The effect of anharmonicity on the classical DOS is large at energies near dissociation, leading to a factor of 5 enhancement in the DOS relative to the harmonic DOS. Because of the more rapid rise of the anharmonic DOS, the contribution to the partition function from energies near dissociation is greater for the anharmonic compared to the harmonic DOS. Imposing the harmonic oscillator constraint on the anharmonic DOS extrapolates the anharmonic DOS above dissociation using the same functional form as for the RRHO DOS. Therefore, the curves for $\rho^{HO}_{CH}(E)$ and $\rho^{HO}_{CA}(E)$ in Figure 4 are parallel above $E = D$ with $\rho^{HO}_{CA}(E)$ shifted up by about a factor of 5. As shown in Table 2, the anharmonic partition functions, $Q^D_{CA}(T)$, are larger than the harmonic ones, $Q^D_{CH}(T)$, by factors of 3.3 to 3.9, and values of $Q^{HO}_{CA}(T)$ are larger than $Q^{HO}_{CH}(T)$ by factors of 3.3 to 4.1. The ratio $Q^{HO}_{CA}(T)/Q^D_{CA}(T)$ is similar in value to $Q^{HO}_{CH}(T)/Q^D_{CH}(T)$, rising from 1.1 to 7.2 as the temperature increases from 200 to 500 K.

Figure 5 provides a comparison of the classical and quantum mechanical DOS in the RRHO approximation. For energies

TABLE 2: Calculated Partition Functions

	temperature (K)						
method	200	250	300	350	400	450	500
$Q^{D}_{CH}(T)$	2.6×10^2	1.2×10^3	3.5×10^3	8.1×10^3	1.5×10^4	2.6×10^4	3.9×10^4
$Q^{D\nu k}_{CH}(T)$, $k = 6$	2.7×10^2	1.4×10^3	4.6×10^3	1.2×10^4	2.7×10^4	5.2×10^4	9.0×10^4
$Q^{D\nu k}_{CH}(T)$, $k = 3$	2.8×10^2	1.5×10^3	5.8×10^3	1.8×10^4	4.7×10^4	1.1×10^5	2.3×10^5
$Q^{HO}_{CH}(T)$	2.8×10^2	1.5×10^3	5.8×10^3	1.9×10^4	5.1×10^4	1.2×10^5	2.7×10^5
$Q^{D}_{CA}(T)$	8.5×10^2	4.1×10^3	1.3×10^4	3.0×10^4	5.8×10^4	9.9×10^4	1.5×10^5
$Q^{HO}_{CA}(T)$	9.3×10^2	5.4×10^3	2.2×10^4	7.3×10^4	2.0×10^5	5.0×10^5	1.1×10^6
$Q^{R}_{CA}(T)$			9.9×10^6		1.7×10^7		
$Q^{D}_{QH}(T)$	6.3×10^1	3.9×10^2	1.4×10^3	3.5×10^3	7.2×10^3	1.3×10^4	2.0×10^4
$Q^{D\nu k}_{QH}(T)$, $k = 6$	7.2×10^1	5.2×10^2	2.2×10^3	6.5×10^3	1.5×10^4	3.1×10^4	5.5×10^4
$Q^{D\nu k}_{QH}(T)$, $k = 3$	7.8×10^1	6.4×10^2	3.2×10^3	1.1×10^3	3.3×10^4	8.2×10^4	1.8×10^4
$Q^{HO}_{QH}(T)$	7.8×10^1	6.4×10^2	3.2×10^3	1.2×10^4	3.6×10^4	9.3×10^4	2.2×10^4

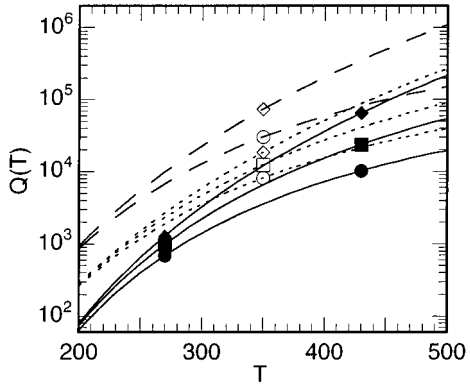

Figure 6. Calculated partition functions for the water dimer using the Dang−Chang interaction model. Dotted and dashed lines and open symbols denote classical partition functions, while solid lines and filled symbols denote quantum mechanical partition functions. The dotted and solid lines indicated calculations that use the RRHO approximation, while the dashed line is for anharmonic calculations. Circles, squares, and diamonds indicate the total energy constraint, vibrational energy constraint with $k = 6$, and harmonic oscillator constraint, respectively, for energies above dissociation. Key: $Q^{D}_{CH}(T)$ (○, dotted line), $Q^{D\nu k}_{CH}(T)$ (□, dotted line), $Q^{HO}_{CH}(T)$ (◇, dotted line), $Q^{D}_{CA}(T)$ (○, dashed line), $Q^{HO}_{CA}(T)$ (◇, dashed line), $Q^{D}_{QH}(T)$ (●, solid line), $Q^{D\nu k}_{QH}(T)$ (■, solid line), $Q^{HO}_{QH}(T)$ (♦, solid line).

below dissociation, the classical density scales as $E^{6.5}$, as shown in eq A.4, rising from zero at $E = 0$. Because of the zero-point energy constraint, the quantum mechanical DOS is zero for energies up to the zero-point energy, which is about 824 cm^{-1} in the RRHO approximation. Just above dissociation, the classical DOS is much larger than the quantum mechanical one, for example, $\rho^{HO}_{CH}(E)/\rho^{HO}_{QH}(E)$ is 3.8 at $E = 1000$ cm^{-1}, and this difference decreases so that at dissociation the ratio is only 1.5. Therefore, the classical DOS appears to be a reasonable approximation to the quantum mechanical one (to within about 50%) for energies above dissociation. The classical partition functions are larger than the analogous quantum mechanical ones, as shown in Table 2. For example $Q^{D}_{CH}(T)/Q^{D}_{QH}(T)$, $Q^{D\nu k}_{CH}(T)/Q^{D\nu k}_{QH}(T)$ for $k = 6$, and $Q^{HO}_{CH}(T)/Q^{HO}_{QH}(T)$ are 4.1, 3.8, and 3.6, respectively, at 200 K and decrease to 2.0, 1.6, and 1.2 at 500 K. Figure 6 displays the same trend, which shows that the classical and quantum mechanical partition functions for a given constraint converge with increasing temperature (compare the solid and dotted curves for the same symbol, such as circle, in Figure 6), whereas the quantum mechanical partition functions for different constraints diverge with increasing temperature (compare the three solid curves in Figure 6). At higher temperatures, the differences between the classical and quantum partition functions are much less than the differences due to different constraints.

4. Summary and Conclusions

In this paper, we examine four different treatments of dissociative states in classical and quantum mechanical calculations of partition functions for the water dimer. Two of the constraints restrict the energy of the system; either the total energy or the vibrational energy is constrained to lie below the dissociation energy. These energy constraints yield the smallest partition functions, with the total energy constraint giving the smallest partition functions of the two. A third constraint uses the rigid rotor harmonic oscillator approximation to extend the calculation of the density of states above the dissociation energy. This constraint imposes no restriction on the total energy of the system but implicitly restricts the phase space of the dimer so that dissociative states are approximated by a discrete spectrum of quantum states rather than by a continuum of states. The fourth constraint restricts the center-of-mass separation of the two water molecules to lie within a constant value. This geometric constraint is only applied to the calculation of classical partition functions and yields the largest partition functions.

For temperatures above 300 K, we find that different constraints lead to differences in the computed partition functions by more than 2 orders of magnitude. The magnitude of these changes is larger than the differences in the classical and quantum mechanical RRHO partition functions, which are typically less than a factor of 8 for temperatures above 300 K. This study shows that for the water dimer at temperatures above 300 K, *the choice of how dissociative states are treated is just as important as an accurate quantum mechanical treatment in evaluating the partition function*. Furthermore, the importance of dissociative states indicates that the accuracy of previous calculations of the dimer partition function[1,4,5,7,9] is highly suspect, because they have either entirely neglected contributions from above dissociation or have implicitly used an untested approximation (e.g., the harmonic approximation) to include contributions from energies above dissociation.

The ambiguity in defining the water dimer partition function indicates that asking questions about the equilibrium population of water dimers without any additional information is ill-posed. Ultimately, we are not interested in knowing the number of water dimers present for some set of physical conditions (i.e., temperature and humidity), but we want to know the effect of

water dimers on a physical observable. For instance, to understand the influence of water dimers on solar absorption requires knowing absorption cross sections for individual states of the dimer and the population of those states. By starting from a rigorous expression for the physical quantity of interest, one could make simplifying approximations that yield an expression for the observable in terms of the concentration of dimers multiplied by a value of the observable that is averaged over different states of the dimer. A careful analysis of the approximations made in the simplified expression could provide insight into what type of constraint is most appropriate for a given physical observable. However, it is not possible to present a general prescription for constraining weakly bound systems, such as the water dimer above 300 K, without any additional information about the physical observable due to the appreciable population of states near the dissociation energy.

Acknowledgment. The authors would like to acknowledge helpful discussions with Richard Saykally, and with Claude Leforestier and Nir Goldman who reviewed an early draft of this work. This work was supported by the Division of Chemical Sciences, Office of Basic Energy Sciences, of the U.S. Department of Energy. This research was performed in the William R. Wiley Environmental Molecular Sciences Laboratory a national scientific user facility sponsored by the Department of Energy's Office of Biological and Environmental Research and located at Pacific Northwest National Laboratory. Pacific Northwest National Laboratory is operated for the Department of Energy by Battelle.

Appendix A. Classical Rigid Rotor Harmonic Oscillator Density of States and Partition Functions

In the RRHO approximation, it is possible to write the classical rovibrational density of states as a convolution of the DOS for classical rigid (CR) rotations and the DOS for classical harmonic (CH) vibrations. The RRHO approximation to the rovibrational DOS, using the third constraint listed above ($y =$ HO), is expressed as

$$\rho_{CH}^{HO}(E) = \int_0^E d\epsilon\, \rho_{CR}^{r}(E-\epsilon)\rho_{CH}^{v}(\epsilon) \tag{A.1}$$

The RRHO approximation is obtained by expanding the potential about one of the eight equivalent minima on the potential energy surface and using unsymmetrized expressions for the rotational partition function. By doing this, the correct symmetry factor of 8 associated with the rotational symmetry of each water molecule and the indistinguishability between the water molecules is properly taken into account. The classical rotational density of state for an asymmetric top is given by

$$\rho_{CR}^{r}(E) = \frac{2(8I_A I_B I_C)^{1/2}}{\hbar^3} E^{1/2} \tag{A.2}$$

where I_A, I_B, and I_C are the principle moments of inertia and $\hbar \equiv h/2\pi$. The classical harmonic vibrational density of state is given by

$$\rho_{CH}^{v}(E) = \frac{E^{M-1}}{(M-1)!}\prod_{m=1}^{M}\frac{1}{\hbar\omega_m} \tag{A.3}$$

where ω_m is the frequency for the mth vibrational mode and $M = 6$ for the intermolecular vibrations of the water dimer. Inserting eqs A.2 and A.3 into eq A.1 yields the result

$$\rho_{CH}^{HO}(E) = E^{M+1/2}\frac{(8I_A I_B I_C)^{1/2}}{\hbar^3} 2\prod_{m=1}^{M}\frac{1}{\left(m+\frac{1}{2}\right)\hbar\omega_m} \tag{A.4}$$

In the RRHO approximation, the partition function for this constraint takes the usual form

$$Q_{CH}^{HO}(T) = Q_{CR}^{r}(T)Q_{CH}^{v}(T) \tag{A.5}$$

where the rotational partition function is given by

$$Q_{CR}^{r}(T) = \frac{(8\pi I_A I_B I_C)^{1/2}}{\hbar^3}(k_B T)^{3/2} \tag{A.6}$$

and the vibrational partition function is given by

$$Q_{CH}^{v}(T) = \prod_{m=1}^{M}\frac{k_B T}{\hbar\omega_m} \tag{A.7}$$

The third constraint is also applied to the anharmonic DOS for energies above dissociation by using the expression

$$\rho_{CA}^{HO}(E) = C_{CA}^{HO}E^{M+1/2}, \quad E > D \tag{A.8}$$

where the constant C_{CA}^{HO} is fitted by matching this expression to $\rho_{CA}^{D}(E)$ at an energy near D. The partition function $Q_{CA}^{HO}(T)$ in this case is obtained by numerical integrating of eq 1 using $\rho_{CA}^{D}(E)$ for energies up to dissociation and $\rho_{CA}^{HO}(E)$ for energies above dissociation.

For the first constraint ($y = D$) given by eq 3, the rovibrational DOS is given by

$$\begin{aligned}\rho_{CH}^{D}(E) &= \theta(D-E)\int_0^E d\epsilon\, \rho_{CR}^{r}(E-\epsilon)\rho_{CH}^{v}(\epsilon) \\ &= \rho_{CH}^{HO}(E)\theta(D-E)\end{aligned} \tag{A.9}$$

and the partition function takes the form

$$Q_{CH}^{D}(T) = Q_{CH}^{r}(T)Q_{CH}^{v}(T) \times \left[\mathrm{erf}(\sqrt{\beta D}) - 2\sqrt{\frac{\beta D}{\pi}}\, e^{-\beta D}\sum_{m=0}^{M}\frac{m!(4\beta D)^m}{(2m+1)!}\right] \tag{A.10}$$

where erf(x) is the error function. The anharmonic partition function for the first constraint, $Q_{CA}^{D}(T)$ is obtained by numerical integration of eq 1, including energies only up to dissociation and using numerically determined values for $\rho_{CA}^{D}(E)$.

For the second constraint ($y = Dvk$) given by eq 4, the rovibrational DOS is written

$$\rho_{CH}^{Dvk}(E) = \rho_{CH}^{HO}(E)\begin{cases}1, & E \le D \\ 1 - \sum_{m=0}^{M-1} C_m^k\left(1-\frac{D}{E}\right)^{m+3/2}, & E > D\end{cases} \tag{A.11}$$

where

$$C_m^k = 0, \quad m = 0, \quad k = 1, ..., M-1$$

$$C_m^k = \frac{(-1)^{M+k+m}}{(k-1)!\left(m+\frac{3}{2}\right)} \prod_{l=1}^{M}\left(l+\frac{1}{2}\right)^{\min(M-k-1,M-m-1)} \sum_{l=0} \frac{1}{l!(M-m-l-1)!} \sum_{n=l}^{\min(M-k-1,m+l-1)} \frac{(-1)^n (M-n-2)!}{(M-k-n-1)!(n-l)!(m+l-n-l)!\left(n-l+\frac{3}{2}\right)},$$

$$m > 0, \quad k = 1, ..., M-1$$

$$C_m^k = \frac{(-1)^m}{(M-m-1)!m!\left(m+\frac{3}{2}\right)} \prod_{l=1}^{M}\left(l+\frac{1}{2}\right), \quad k = M \quad \text{(A.12)}$$

The partition function with this constraint is given by

$$Q_{CH}^{Dvk}(T) = Q_{CH}^{r}(T) Q_{CH}^{v}(T)\left[1 - e^{-\beta D} \sum_{m=0}^{k-1} \frac{(\beta D)^m}{m!}\right] \quad \text{(A.13)}$$

Note that this constraint is only applied with the RRHO approximation.

Appendix B. Quantum Mechanical Rigid Rotor Harmonic Oscillator Density of States and Partition Functions

The quantum mechanical partition function in the RRHO approximation, using the third constraint (y = HO), is given by an expression analogous to eq A.1

$$\rho_{QH}^{HO}(E) = \int_0^E d\epsilon\, \rho_{QR}^{r}(E-\epsilon)\rho_{QH}^{v}(\epsilon) \quad \text{(B.1)}$$

where the vibrational DOS in the harmonic approximation is given by

$$\rho_{QH}^{v}(E) = \sum_{n_1=0}^{\infty}\sum_{n_2=0}^{\infty} ... \sum_{n_M=0}^{\infty} \delta(E - \sum_{m=1}^{M} \epsilon_{n_m}^{v}) = \sum_{\mathbf{n}=0}^{\infty} \delta(E - \epsilon_{\mathbf{n}}^{v}) \quad \text{(B.2)}$$

the collection of vibrational quantum numbers is denoted by $\mathbf{n} = (n_1, n_2, ..., n_M)$, the vibrational energy levels in mode m are given by

$$\epsilon_{n_m}^{v} = \hbar\omega_m(n_m + (1/2)) \quad \text{(B.3)}$$

and the total vibrational energy for state $\mathbf{n}$ is denoted

$$\epsilon_{\mathbf{n}}^{v} = \sum_{m=1}^{M} \epsilon_{n_m}^{v} \quad \text{(B.4)}$$

For the prolate symmetric top energy levels and degeneracies given by eq 7, the rotational DOS is given by

$$\rho_{QR}^{r}(E) = \sum_{J=0}^{\infty}(2J+1)\sum_{K=0}^{J}(2-\delta_{K,0})\delta(E-\epsilon_{JK}^{r}) \quad \text{(B.5)}$$

where $\delta_{K,K'}$ is the Kronecker delta function and the rotational energy levels are given by eq 7. Substituting eq B.2 into B.1 yields

$$\rho_{QH}^{HO}(E) = \sum_{n_1=0}^{\infty}\sum_{n_2=0}^{\infty} ... \sum_{n_M=0}^{\infty} \rho_{QR}^{r}(E - \sum_{m=1}^{M}\epsilon_{n_m}^{v}) = \sum_{\mathbf{n}=0}^{\infty} \rho_{QR}^{r}(E - \epsilon_{\mathbf{n}}^{v}) \quad \text{(B.6)}$$

and the partition function is then obtained using eq B.6 in eq 1 to give

$$Q_{QH}^{HO}(T) = Q_{QR}^{r}(T) Q_{QH}^{v}(T) \quad \text{(B.7)}$$

The rigid rotor approximation to the rotational partition function $Q_{QR}^{r}(T)$ is given by

$$Q_{QR}^{r}(E) = \sum_{J=0}^{\infty}(2J+1)\sum_{K=0}^{J}(2-\delta_{K,0})\exp(-\epsilon_{JK}^{r}/k_B T) \quad \text{(B.8)}$$

and the quantum mechanical HO partition function for vibrations is the standard expression

$$Q_{QH}^{v}(E) = \prod_{m=1}^{M} \frac{1}{2\sinh(\hbar\omega_m/(2k_B T))} \quad \text{(B.9)}$$

As mentioned above, calculating the DOS by a direct sum over energy levels is impractical, so we explore the validity of the classical approximation to the rotational DOS.

It is convenient to compare the classical and quantum mechanical number of rotational states. The quantum mechanical number of rotational states is defined by

$$N_{QR}^{r}(E) = \int_0^E d\epsilon\, \rho_{QR}^{R}(\epsilon) = \sum_{J=0}^{\infty}(2J+1)\sum_{K=0}^{J}(2-\delta_{K,0})\theta(E-\epsilon_{JK}^{r}) \quad \text{(B.10)}$$

and classically, it is given by

$$N_{CR}^{r}(E) = \frac{4(8I_A I_B I_C)^{1/2}}{3\hbar^3} E^{3/2} \quad \text{(B.11)}$$

Numerical comparisons of N_{QR}^{r} and N_{CR}^{r} are shown in Figure 5 and discussed above. We approximate $\rho_{QH}^{HO}(E)$ using eq B.6 with ρ_{QR}^{r} replaced by ρ_{CR}^{r}

$$\rho_{QH}^{HO}(E) \approx \sum_{n_1=0}^{\infty}\sum_{n_2=0}^{\infty} ... \sum_{n_M=0}^{\infty} \rho_{CR}^{r}(E - \sum_{m=1}^{M}\epsilon_{n_m}^{v}) = \sum_{\mathbf{n}=0}^{\infty} \rho_{CR}^{r}(E - \epsilon_{\mathbf{n}}^{v}) \quad \text{(B.12)}$$

and the total RRHO partition function is approximated by

$$Q_{QH}^{HO}(T) \approx Q_{CR}^{r}(T) Q_{QH}^{v}(T) \quad \text{(B.13)}$$

Equation B.12 is the starting point for examining the effects of the energy constraint on the partition function.

The RRHO quantum mechanical DOS with the total energy constraint ($y = D$) is approximated by

$$\rho_{QH}^{D}(E) \approx \theta(D-E)\rho_{QH}^{HO}(E) \quad \text{(B.14)}$$

and the partition function with this constraint is given by

$$Q_{\mathrm{QH}}^{D}(T) \approx Q_{\mathrm{CR}}^{\mathrm{r}}(T)\sum_{\mathbf{n}=0}^{\infty}\theta(D-\epsilon_{\mathbf{n}}^{\mathrm{v}})\exp(-\epsilon_{\mathbf{n}}^{\mathrm{v}}/(k_{\mathrm{B}}T))\times \left[\mathrm{erf}\left(\sqrt{\frac{D-\epsilon_{\mathbf{n}}^{\mathrm{v}}}{k_{\mathrm{B}}T}}\right)-2\sqrt{\frac{D-\epsilon_{\mathbf{n}}^{\mathrm{v}}}{\pi k_{\mathrm{B}}T}}\exp\left(-\frac{D-\epsilon_{\mathbf{n}}^{\mathrm{v}}}{k_{\mathrm{B}}T}\right)\right] \quad \text{(B.15)}$$

The RRHO quantum mechanical DOS with the vibrational energy constraint ($y = D\nu k$) requires specification of the k modes. For convenience, we take these to be the mode $m = 1, ..., k$. With this definition, the DOS is given by

$$\rho_{\mathrm{QH}}^{D\nu k}(E) = \sum_{n_1=0}^{\infty}\sum_{n_2=0}^{\infty}\cdots\sum_{n_M=0}^{\infty}\rho_{\mathrm{CR}}^{\mathrm{r}}(E-\sum_{m=1}^{M}\epsilon_{n_m}^{\mathrm{v}})\theta(D-\sum_{m=1}^{k}\epsilon_{n_m}^{\mathrm{v}})$$

$$= \sum_{\mathbf{n}=0}^{\infty}\rho_{\mathrm{CR}}^{\mathrm{r}}(E-\epsilon_{\mathbf{n}}^{\mathrm{v}})\theta(D-\epsilon_{\mathbf{n}}^{\nu k}) \quad \text{(B.16)}$$

where we define the vibrational energy in the k modes as

$$\epsilon_{\mathbf{n}}^{\nu k} = \sum_{m=1}^{k}\epsilon_{n_m}^{\mathrm{v}} \quad \text{(B.17)}$$

The partition function for this method takes the form

$$Q_{\mathrm{QH}}^{D\nu k}(T) \approx Q_{\mathrm{CR}}^{\mathrm{r}}(T)\left[\prod_{m=k+1}^{M}\frac{1}{2\sinh(\hbar\omega_m/(2k_{\mathrm{B}}T))}\right]\times \sum_{n_1=0}^{\infty}\sum_{n_2=0}^{\infty}\cdots\sum_{n_k=0}^{\infty}\theta(D-\sum_{m=1}^{k}\epsilon_{n_m}^{\mathrm{v}})\exp(-\sum_{m=1}^{k}\epsilon_{n_m}^{\mathrm{v}}/(k_{\mathrm{B}}T)),$$

$$k = 1, ..., M-1$$

$$Q_{\mathrm{QH}}^{D\nu k}(T) \approx Q_{\mathrm{CR}}^{\mathrm{r}}(T)\sum_{\mathbf{n}=0}^{\infty}\theta(D-\epsilon_{\mathbf{n}}^{\mathrm{v}})\exp(-\epsilon_{\mathbf{n}}^{\mathrm{v}}/(k_{\mathrm{B}}T)), \quad k = M \quad \text{(B.18)}$$

References and Notes

(1) Salnina, Z.; Crifo, J. F. *Int. J. Thermophys.* **1992**, *13*, 465. Tso, W.; Geldart, D. J. W.; Chylek, P. *J. Chem. Phys.* **1998**, *108*, 5319.

(2) Devir, A. D.; Neumann, M.; Lipson, S. G.; Oppenheim, U. P. *Opt. Eng.* **1994**, *33*, 746. Akhmatskaya, E. V.; Apps, C. J.; Hillier, I. H.; Masters, A. J.; Watt, N. E.; Whitehead, J. C. *Chem. Commun.* **1997**, *707*. Daniel, J. S.; Solomon, S.; Sanders, R. W.; Portmann, R. W.; Miller, D. C.; Madsen, W. *J. Geophys. Res., [Atmos.]* **1999**, *104*, 16785. Arking, A. *Science* **1996**, *273*, 779. Arking, A. *Geophys. Res. Lett.* **1999**, *26*, 2729. Arking, A. J. *Climate* **1999**, *12*, 1589.

(3) Pilewskie, P.; Valero, F. P. J. *Science* **1995**, *267*, 1626. Chylek, P.; Fu, Q.; Tso, W.; Geldart, D. J. W. *Tellus* **1999**, *51A*, 304.

(4) Chylek, P.; Geldart, D. J. W. *Geophys. Res. Lett.* **1997**, *24*, 2015.

(5) Vaida, V.; Headrick, J. E. *J. Phys. Chem. A* **2000**, *104*, 5401.

(6) Keyes, F. G. *J. Chem. Phys.* **1947**, *15*, 602. Kell, G. S.; McLaurin, G. E.; Whalley, E. *J. Chem. Phys.* **1968**, *48*, 3805. Dymond, J. H.; Smith, E. B. *The Virial Coefficients of Gases*; Clarendon: Oxford, U.K., 1969. Gebbie, H. A.; Burroughs, W. J.; Chamberlain, J.; Harries, J. E.; Jones, R. G. *Nature (London)* **1969**, *221*, 143. Curtiss, L. A.; Frurip, D. J.; Blander, M. *J. Chem. Phys.* **1979**, *71*, 2703. Dianov-Klokov, V. I.; Ivanov, V. M.; Arefev, V. N.; Sizov, N. I. *J. Quant. Spectrosc. Radiat. Transfer* **1981**, *25*, 83. Bondarenko, G. V.; Gorbaty, Y. E. *Mol. Phys.* **1991**, *74*, 639.

(7) Kim, K. S.; Mhin, B. J.; Choi, U.-S.; Lee, K. *J. Chem. Phys.* **1992**, *97*, 6649. Mhin, B. J.; Lee, S. J.; Kim, K. S. *Phys. Rev. A* **1993**, *48*, 3764. Munoz-Caro, C.; Nino, A. *J. Phys. Chem. A* **1997**, *101*, 4128. Hobza, P.; Bludsky, O.; Suhai, S. *Phys. Chem. Chem. Phys.* **1999**, *1*, 3073.

(8) Schenter, G. K. *J. Chem. Phys.* **1998**, *108*, 6222.

(9) Goldman, N.; Fellers, R. S.; Leforestier, C.; Saykally, R. J. *J. Phys. Chem. A* **2001**, *105*, 515.

(10) Fellers, R. S.; Braly, L. B.; Saykally, R. J.; Leforestier, C. *J. Chem. Phys.* **1999**, *110*, 6306.

(11) Fellers, R. S.; Leforestier, C.; Braly, L. B.; Brown, M. G.; Saykally, R. J. *Science* **1999**, *284*, 945.

(12) Schenter, G. K.; Kathmann, S. M.; Garrett, B. C. *Phys. Rev. Lett.* **1999**, *82*, 3484.

(13) Schenter, G. K.; Kathmann, S. M.; Garrett, B. C. *J. Chem. Phys.* **1999**, *110*, 7951. Kathmann, S. M.; Schenter, G. K.; Garrett, B. C. *J. Chem. Phys.* **1999**, *111*, 4688.

(14) Leforestier, C.; Braly, L. B.; Kun, L.; Elrod, M. J.; Saykally, R. J. *J. Chem. Phys.* **1997**, *106*, 8527. Carter, S.; Culik, S. J.; Bowman, J. M. *J. Chem. Phys.* **1997**, *107*, 10458. Carter, S.; Bowman, J. M. *J. Chem. Phys.* **1998**, *108*, 4397.

(15) Christoffel, K. M.; Bowman, J. M. *J. Phys. Chem. A* **1999**, *103*, 3020.

(16) Stillinger, F. H. *J. Chem. Phys.* **1963**, *38*, 1486.

(17) Reiss, H.; Katz, J. L.; Cohen, E. T. *J. Chem. Phys.* **1968**, *48*, 5553.

(18) Lee, J. K.; Barker, J. A.; Abraham, F. F. *J. Chem. Phys.* **1973**, *58*, 3166.

(19) Rao, M.; Berne, B. J.; Kalos, M. H. *J. Chem. Phys.* **1978**, *68*, 1325. Reiss, H.; Tabazadeh, A.; Talbot, J. *J. Chem. Phys.* **1990**, *92*, 1266. Ellerby, H. M.; Weakliem, C. L.; Reiss, H. *J. Chem. Phys.* **1991**, *95*, 9209. Ellerby, H. M.; Weakliem, C. L.; Reiss, H. *J. Chem. Phys.* **1992**, *97*, 5766. Weakleim, C. L.; Reiss, H. *J. Chem. Phys.* **1993**, *99*, 5374. Weakliem, C. L.; Reiss, H. *J. Chem. Phys.* **1994**, *101*, 2398.

(20) Eyring, H. *Trans. Faraday Soc*. **1938**, *34*, 41. Eyring, H. *J. Chem. Phys* **1935**, *3*, 107. Wigner, E. *Trans. Faraday Soc.* **1938**, *34*, 29.

(21) Baer, T.; Hase, W. L. *Unimolecular Reaction Dynamics*; Oxford University Press: New York, 1996.

(22) Chandler, D. *J. Chem. Phys.* **1978**, *68*, 2959.

(23) Truhlar, D. G.; Garrett, B. C.; Klippenstein, S. J. *J. Phys. Chem.* **1996**, *100*, 12771.

(24) Berblinger, M.; Schlier, C. *J. Chem. Phys.* **1994**, *101*, 4750.

(25) Remacle, F.; Levine, R. D. *J. Phys. Chem.* **1996**, *100*, 7962.

(26) Smith, F. T. *J. Chem. Phys.* **1963**, *38*, 1034.

(27) Smith, F. T. *Phys. Rev.* **1960**, *118*, 349.

(28) Kinsey, J. L. *Chem. Phys. Lett.* **1971**, *8*, 349.

(29) Brumer, P.; Fitz, D. E.; Wardlaw, D. *J. Chem. Phys.* **1980**, *72*, 386.

(30) Roberts, R. E.; Bernstein, R. B.; Curtiss, C. F. *J. Chem. Phys.* **1969**, *50*, 5163. Bowman, J. M. *J. Phys. Chem.* **1986**, *90*, 3492.

(31) Pack, R. T.; Butcher, E. A.; Parker, G. A. *J. Chem. Phys.* **1995**, *102*, 5998.

(32) Dang, L. X.; Chang, T. M. *J. Chem. Phys.* **1997**, *106*, 8149.

(33) Weerasinghe, S.; Amar, F. G. *J. Chem. Phys.* **1993**, *98*, 4967. Bichara, C.; Gaspard, J.-P.; Mathieu, J.-C. *J. Chem. Phys.* **1988**, *89*, 4339. Ferrenberg, A. M.; Swendson, R. H. *Phys. Rev. Lett.* **1989**, *63*, 1195. Labastie, P.; Whetten, R. L. *Phys. Rev. Lett.* **1990**, *65*, 1567.